# Optically Engineering the Topological Properties of a Spin Hall Insulator

Balázs Dóra,[1,2,*] Jérôme Cayssol,[3,4,5] Ferenc Simon,[1] and Roderich Moessner[4]

[1]*Department of Physics, Budapest University of Technology and Economics, Budafoki út 8, 1111 Budapest, Hungary*
[2]*BME-MTA Exotic Quantum Phases Research Group, Budapest University of Technology and Economics, Budapest, Hungary*
[3]*LOMA (UMR-5798), CNRS and University Bordeaux 1, F-33045 Talence, France*
[4]*Max-Planck-Institut für Physik komplexer Systeme, Nöthnitzer Strasse 38, 01187 Dresden, Germany*
[5]*Department of Physics, University of California, Berkeley, California 94720, USA*

(Received 14 June 2011; published 31 January 2012)

Time-periodic perturbations can be used to engineer topological properties of matter by altering the Floquet band structure. This is demonstrated for the helical edge state of a spin Hall insulator in the presence of monochromatic circularly polarized light. The inherent spin structure of the edge state is influenced by the Zeeman coupling and not by the orbital effect. The photocurrent (and the magnetization along the edge) develops a finite, helicity-dependent expectation value and turns from dissipationless to dissipative with increasing radiation frequency, signalling a change in the topological properties. The connection with Thouless' charge pumping and nonequilibrium zitterbewegung is discussed, together with possible experiments.

DOI: 10.1103/PhysRevLett.108.056602 PACS numbers: 72.25.Dc, 03.65.Vf, 75.76.+j, 81.05.ue

*Introduction.*—Topological insulators (TIs) are a focus of attention, not least due to their possible application in spintronics and quantum computation. They represent distinct states of matter with robust, topologically protected conducting helical edge or surface states [1,2]. The importance of the spin-orbit interaction is reflected in their charge carriers having their spin locked to their momentum. In particular, the two-dimensional TI, namely, the quantum spin Hall (QSH) state, has been predicted for a variety of systems including graphene [3], HgTe/CdTe [4], and InAs/GaSb [5] quantum wells, lattice models [6–8], and multicomponent ultracold fermions in optical lattices [9–11]. Nevertheless, in all of these, the gapless helical edge state originates from a subtle band inversion [1,2] which requires careful Bloch band structure engineering [3–11] as well as a high degree of sample control [12–14].

Bloch states and energy bands arise from spatially periodic Hamiltonians in condensed matter systems. Extending the periodicity in the time domain through a time-periodic perturbation increases tunability of the Hamiltonian: The temporal analog of Bloch states (the Floquet states) can be manipulated via the periodicity and amplitude of the external perturbation.

Recently, topological phases of periodically driven quantum systems have been characterized [15] by using Floquet theory, extending the time-independent topological classification [16–18]. Interestingly, novel topological edge states can be induced by shining electromagnetic radiation on a topologically trivial insulator, e.g., a noninverted HgTe/CdTe quantum well with no edge state in the static limit [19]. Besides, a time-dependent perturbation may also be harmful for the coherence of the edge or surface states of TIs by introducing dissipation. It is therefore natural to investigate to what extent the steady state of a TI remains robust against time-dependent perturbations and how the electrical and magnetic properties are altered.

In this work, we consider the one-dimensional helical edge state of a QSH insulator in a circularly polarized radiation field. When increasing the radiation frequency, the steady edge state is found to switch from a dissipationless charge pumping to a dissipative transport regime. We characterize those regimes by their dc and ac photocurrent responses and provide experimental proposals to measure them. Finally, we demonstrate that the photocurrent, the magnetization, and the zitterbewegung phenomenon are ruled by the very same unit vector, whose winding number determines a topological invariant for the system. Although our predictions could be tested by experiments similar to those in graphene [20] and HgTe/CdTe quantum wells [21], they rely on a different coupling mechanism, that is, Zeeman coupling rather than orbital coupling.

*Model.*—We consider a QSH insulator located in the $xy$ plane and irradiated by a circularly polarized electromagnetic field $\mathbf{A}(t) = A_0(\cos(\omega t - kz), \sin(\omega t - kz))$ with wave vector $k$ and frequency $\omega$, whose sign determines the helicity of the polarization (Fig. 1). The time-dependent Hamiltonian of the QSH edge reads [22]

$$H(t) = v_F \sigma^z [p - eA_x(t)] + g[\sigma^+ e^{-i\omega t} + \text{H.c.}], \quad (1)$$

where $\boldsymbol{\sigma}$ is the vector of Pauli matrices representing the physical spin of the electron, $p$ the momentum along the one-dimensional channel, $v_F$ the Fermi velocity, and $e$ the electron charge. The electric current operator [23] is $j = ev_F\sigma^z$. The circularly polarized radiation acts both on the orbital motion through the vector potential $A_x(t) = A_0 \cos\omega t$ and on the electron spin through the Zeeman coupling $g = g_{\text{eff}}\mu_B B_0$, $g_{\text{eff}}$ being the effective $g$ factor

 

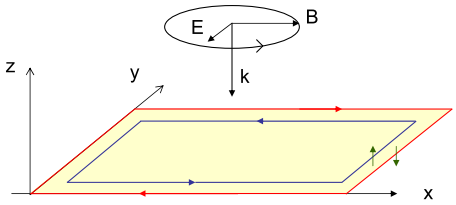


FIG. 1 (color online). The quantum spin Hall insulator (light yellow rectangle) with its helical edge state (counterpropagating red and blue arrows) in a circularly polarized electromagnetic field with frequency $\omega$ and wave vector $k$. In the plane $z = 0$, the rotating magnetic field $\mathbf{B}(t) = B_0(\cos\omega t, \sin\omega t)$ is perpendicular to the $\sigma^z$ direction (vertical green arrows). A small tilting from the $z$ axis does not influence our results.

and $\mu_B$ the Bohr magneton. Nevertheless, at high frequency, the orbital effect can be safely neglected according to a simple semiclassical argument (for a more rigorous treatment, see [23]). An electron traveling at the speed $v_F$ in an electric field $E_0 = A_0\omega = cB_0$ ($c$ the speed of light) during a time $1/\omega$ picks up an energy $v_F eE_0/\omega$ from the vector potential which has to be compared to the smallest energy quantum it can absorb, $\hbar\omega$ (restoring original units). Hence, in the regime $v_F eE_0/\omega \ll \hbar\omega$, only the time-dependent Zeeman effect is effective, and in this respect, our effective Hamiltonian differs significantly from other studies on similar systems [24–31] with a dominant orbital effect. For typical parameters ($v_F = 10^5$ m/s, laser power of 1 mW focused onto an area of 1 mm$^2$, yielding $E_0 \approx 600$ V/m), this requires $\omega \gg 0.5$ THz, i.e., lasers operating in the far infrared or in the visible range. We also assume that $\hbar\omega$ is smaller than the bulk gap of the 2D insulator.

*Floquet states.*—In order to study the steady state of the edge, we solve the time-dependent Schrödinger equation $i\partial_t\Psi_p(t) = H(t)\Psi_p(t)$, with $A_x = 0$ in Eq. (1). By applying Floquet theory [32,33], the solution of the time-dependent Schrödinger equation is written as

$$\Psi_p(t) = \exp[-iE_\alpha(p)t]\Phi_\alpha(p, t), \tag{2}$$

where $E_\alpha(p)$ is the Floquet quasienergy and $\Phi_\alpha(p, t) = \Phi_\alpha(p, t + T)$ with $T = 2\pi/\omega$. From this, physically equivalent steady states can be created [32] by shifting the quasienergy $E_{n,\alpha}(p) = E_\alpha(p) + n\omega$ and defining $\Phi_{n,\alpha}(p, t) = \Phi_\alpha(p, t)\exp(in\omega)$, where $n$ is a relative integer. Then, the quasienergy and wave function are obtained as

$$E_\alpha(p) = \frac{\omega}{2} + \alpha\lambda, \tag{3}$$

$$\Phi_\alpha(p, t) = \frac{1}{\sqrt{2\lambda}}\begin{pmatrix} \sqrt{\lambda + \alpha(v_F p - \omega/2)} \\ \alpha\exp(i\omega t)\sqrt{\lambda - \alpha(v_F p - \omega/2)} \end{pmatrix}, \tag{4}$$

where $\alpha = \pm 1$ and $\lambda = \sqrt{g^2 + (v_F p - \omega/2)^2}$. The quasienergies describe the opening of a gap of size $g$ around $\omega/2$ [23]. This photoinduced gap is located at momentum $p = \omega/2v_F$ and stems from one-photon assisted processes. A given $\Psi_\alpha(p, t)$ describes the steady state where an initial state with $g = 0$ would evolve adiabatically if we switch on the magnetic field at $t = -\infty$.

We introduce the average energy [33], which is used to identify the filled Floquet states [27], in analogy to the stationary situation [23], as

$$\bar{E}_\alpha(p) = \Psi_p^+(t)H\Psi_p(t) = \alpha\left[\lambda + \frac{\omega(v_F p - \omega/2)}{2\lambda}\right], \tag{5}$$

which is always single-valued as opposed to the ladder of quasienergies $E_{n,\alpha}(p)$.

*High- and low-frequency regimes.*—It is natural to distinguish high and low frequencies in terms of the ratio of the Zeeman coupling strength $g$ and radiation frequency $\omega$. More specifically, the Floquet spectrum happens to be gapped for $|\omega| < 4g$ and gapless for $|\omega| > 4g$. In the low-frequency regime, the bands are well separated by the photoinduced gap for any momentum, the ($\alpha = -1$) band being the fully occupied one. In contrast, in the high-frequency regime ($|\omega| > 4g$), the states of the ($\alpha = +1$) band become lower in energy than the ones of the ($\alpha = -1$) band within the momenta range $\omega_- < v_F p < \omega_+$ with $4\omega_\pm = \omega \pm \sqrt{\omega^2 - 16g^2}$ [23]. The band touching at $|\omega| = 4g$ has a clear signature in the total energy which picks up a singular contribution as

$$E_{\text{tot}} = E_s(g, \omega) + \frac{\rho_0\sqrt{g}}{3}(|\omega| - 4g)^{3/2} \tag{6}$$

for $|\omega| \gtrsim 4g$, while $E_s(g, \omega) = \rho_0[\omega^2/4 - g^2\ln(2W\sqrt{e}/g)]$ is a *smooth* function of $(\omega - 4g)$. The lattice constant is denoted by $a$, $\rho_0 = a/\pi v_F$, and $W$ is a high energy cutoff. The exponent $3/2$ appears also in the orbital contribution to the ground state energy of two-dimensional Dirac fermions [34].

*Electromagnetic response and topological invariants.*—The electromagnetic response of the QSH edge state is more easily detected than the singularity in the ground state energy Eq. (6). As a main signature, a dc photocurrent $\langle j\rangle$ is generated along the edge whose direction is determined by the helicity of the circular polarization. Interestingly, there is no accompanying ac current in the absence of orbital coupling. Moreover, the current operator being $j = ev_F\sigma^z$, such a dc current also corresponds to a steady-state magnetization $\langle\sigma^z\rangle$ along the edge.

We have obtained the full dependence of the dc-photocurrent or steady-state magnetization for any arbitrary frequency within the bulk gap of the QSH insulator. Besides, we demonstrate that the dc photocurrent is directly related to a topological property of the time-dependent Floquet state, that is, the topological invariant:

$$C_\alpha = \frac{1}{2}\sum_p \int_0^T dt \hat{\mathbf{d}}_{\alpha,p}(t)\cdot[\partial_p \hat{\mathbf{d}}_{\alpha,p}(t)\times\partial_t \hat{\mathbf{d}}_{\alpha,p}(t)]. \quad (7)$$

This Chern number $\mathcal{C}_\alpha$, associated with the band $\alpha$, is the winding number of the mapping, $(p,t)\to\hat{\mathbf{d}}_{\alpha,p}(t) = \Phi_\alpha^+(p,t)\boldsymbol{\sigma}\Phi_\alpha(p,t) = \alpha(g\cos\omega t, g\sin\omega t, v_F p - \omega/2)/\lambda$, between the $(1+1)$-dimensional extended Brillouin zone in $(p,t)$ space and the unit sphere [1,19], the summation being taken over occupied bands.

*In the low-frequency regime* ($|\omega| < 4g$), the dc photocurrent

$$\langle j\rangle = \int_{-\infty}^{\infty} \frac{e v_F dp}{2\pi}\hat{\mathbf{d}}^z_{-,p}(t) = \frac{e\omega}{2\pi}, \quad (8)$$

is independent of the coupling strength $g$, the charge pumped within one cycle ($T$) being exactly the unit charge. This adiabatic pumped current has been considered in Ref. [22]. As noticed by Thouless [35], the integer charge pumped across a 1D insulator in one period of an (adiabatic) cycle is a topological invariant that characterizes the cycle. Here this specific quantization of charge stems directly from the quantized Chern number

$$C_\alpha = -\int_{-\infty}^{\infty} dp \frac{\alpha\,\mathrm{sgn}(\omega) v_F g^2}{2\lambda^3} = -\alpha\,\mathrm{sgn}(\omega), \quad (9)$$

the ground state being the filled $\alpha = -1$ band, yielding $\langle j\rangle = e\mathcal{C}_-/T$. The dc current is therefore dissipationless, protected by a photoinduced gap [23].

*At high frequency* $|\omega| > 4g$, the system undergoes a photoinduced band inversion and the Chern number

$$C_\alpha = -\alpha\,\mathrm{sgn}(\omega)\left(1 - \sum_{s=\pm1} s\frac{\sqrt{2\omega\omega_s}}{\omega}\right) \quad (10)$$

is no longer quantized (Fig. 2), reminiscent of the transfer of the Chern number between equilibrium bands which touch. We note that the Chern number is continuous at the transition $|\omega| = 4g$ and vanishes slowly as $\mathcal{C}_\alpha = -\alpha 2g/\omega$ for $|\omega| \gg g$.

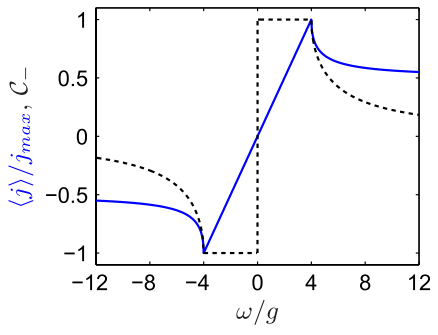


FIG. 2 (color online). The induced photocurrent (blue solid line) and the $\mathcal{C}_-$ Chern number (black dashed line) are shown as a function of the frequency $\omega$. The photocurrent roughly behaves as $\langle j\rangle \approx e\,\mathrm{sgn}(\omega)\min(g, |\omega|/2)/\pi$, and it is maximal at the transition $|\omega| = 4g$ between the low- and the high-frequency regimes. The Chern number becomes nonquantized when band touching occurs at $4g = |\omega|$.

The corresponding dc photocurrent is

$$\langle j\rangle = \frac{e}{2\pi}\left(\omega - \sum_{s=\pm1} s\sqrt{2\omega\omega_s}\right). \quad (11)$$

While the current still satisfies $\langle j\rangle = e\mathcal{C}_-/T$ for $|\omega| > 4g$, it is dissipative and no longer quantized due to the band touching, in analogy with the photovoltaic Hall effect [24] in graphene. The photocurrent approaches the finite asymptotic value $\langle j\rangle = eg\,\mathrm{sgn}(\omega)/\pi$ for $|\omega| \gg g$, which can be regarded as the lowest-order, linear response correction to the current in $g$, hence the weak-coupling regime (Fig. 2).

*Proposal for a measurement setup.*—In practice, the weak-coupling regime $g \ll |\omega|$ is usually realized. There a typical radiation field (magnetic field strength of the order of $10^{-4}$–$10^{-5}$ T) yields a photocurrent of the order of 0.1–10 pA, depending on the effective $g$-factor values, which can be significantly enhanced ($g_{\mathrm{eff}} \approx 20$–$50$) for materials with strong spin-orbit coupling like HgTe/CdTe, InAs/GaSb, HgSe, or $Bi_2Se_3$. Such induced current can be detected in a contactless measurement. When the total area of the QSH insulator is exposed to the radiation field (i.e., the laser's spot size is bigger than the area of the sample), a circulating loop current flows around the sample as in Fig. 1. A perpendicular magnetic field is induced according to the Biot-Savart law as $B_{\mathrm{ind}} = \mu_0 2\sqrt{2}\langle j\rangle/\pi L$, with $L$ the linear size of a square-shaped sample ($\mu_0$ the vacuum permeability), staying roughly constant within the sample. For $\langle j\rangle = 1$ pA and $L = 1$ $\mu$m, this gives $B_{\mathrm{ind}} = 1$ pT. This induced magnetic field is within the detectability limit of an ac SQUID [23]. Finally, standard 2-contacts measurement can also be used in order to detect the photocurrent. For a strip sample with a laser spot size bigger than the width but smaller than the length, backscattering is induced [29], which suppresses the photocurrent.

So far, we have considered the idealistic situation for the generation of the dc photocurrent, namely, zero chemical potential in the QSH edge modes, strictly vanishing orbital effect, and no inversion symmetry breaking. In the following, we discuss how additional effects may influence the dc photocurrent (see also [23]).

*Orbital effect and ac-current response.*—When the vector potential is taken into account (in the typical $v_F eA_0/\omega \ll 1$ regime), an ac current develops on top of the dc one as $\langle j\rangle \approx j_{\mathrm{dc}} + j_{\mathrm{ac}}\cos(\omega t)$. We have solved Eq. (1) numerically [23] with the vector potential, and the results are shown in Fig. 3. The induced ac component stays always small compared to the dc one, because the vector potential without the Zeeman term cannot cause spin-flip processes and is unable to generate any current. Indeed, the matrix element for optical transitions due to the vector potential is $\Phi_+^+(p,t)\sigma^z\Phi_-(p,t) = g/\lambda$. Therefore,

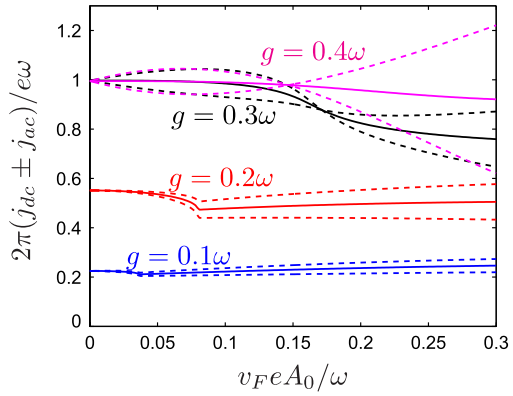


FIG. 3 (color online). The induced dc (by the Zeeman term, solid line) ± the ac (by the vector potential, dashed lines) currents are plotted as a function of the vector potential, for several values of $g$; $j_{ac}$ is always smaller than $j_{dc}$ for physically relevant parameters. The current behaves as $\langle j \rangle \approx j_{dc} + j_{ac}\cos(\omega t)$.

the extended Kubo formula [27] predicts the scaling of the ac component as $j_{ac} \sim v_F eA_0$ [23].

*Effect of the finite doping on the edge.*—So far, we have considered the optimal situation for photocurrent generation, namely, zero Fermi energy in the QSH state. In the case of a finite chemical potential, the dc photocurrent vanishes gradually as we move away from half filling of the QSH edge states. The one-dimensional momentum acts as a polarizing effective magnetic field in Eq. (1). For large momenta $|p| \gg (|\omega|, |g|)/v_F$, this polarization is so strong that the circularly polarized magnetic field hardly induces any magnetization, while close to the Dirac point ($p \sim 0$), the magnetic field represented by the momentum is very weak, and the circularly polarized field dominates over the momentum. The induced, helicity-dependent magnetization originates from these states living close to $p = \omega/2v_F$, as indicated by the nontrivial Aharonov-Anandan phase in this region [23].

*Inversion symmetry breaking and static magnetic field.*—We also consider the effect of a perturbation $g_0\sigma_x$ in the Hamiltonian Eq. (1) in order to mimic an eventual inversion symmetry breaking [22] and subsequent $S^z$ nonconservation (as in HgTe/CdTe quantum wells). This static Zeeman term opens a gap at $p = 0$, whereas the dc current is mainly built up from states near $p = \omega/2v_F$. Therefore, the effect of inversion symmetry breaking on the dc photocurrent is expected to be weak. Indeed, we have checked that the dc current and also the ac component (in the presence of an orbital effect) are almost identical to those of Fig. 3 for $g_0 < g$ [23].

*Zitterbewegung.*—The trembling motion of the center of mass coordinate is caused by interference between the positive and negative energy states (i.e., interband transitions) [36]. The topological invariant measures it indirectly through $\hat{\mathbf{d}}_{\alpha,p}(t)$ in Eq. (7). The position operator satisfies $\partial_t x = v_F\sigma^z =: v(t)$. Generalizing Ref. [36] to nonequilibrium Floquet states, we find

$$\frac{v(t)}{v_F} = \{[\mathbf{n}\circ\mathbf{n} + (\mathbb{1} - \mathbf{n}\circ\mathbf{n})\cos(2\lambda\tilde{t}) + \sin(2\lambda\tilde{t})\mathbf{n}\times]\boldsymbol{\sigma}_0\}_z \quad (12)$$

where $\mathbf{n} = \hat{\mathbf{d}}_{\alpha,p}(t_0)$, $\tilde{t} = t - t_0$, $\mathbf{n}\circ\mathbf{n}$ is the dyadic product, and $\boldsymbol{\sigma}_0$ is the spin configuration at $t = t_0$.

*Conclusion.*—Radiation of a helical edge drives a transition between nondissipative charge pumping at low frequency and a high-frequency dissipative regime, reflected in the behavior of the photocurrent. Note that, for (neutral) atoms in optical traps, one can introduce a Zeeman term without any orbital counterpart or fabricate chiral edge states with spin quantized parallel to the momentum [11]: Without any vector potential, the full transition from dissipationless to dissipative charge pumping can then be followed.

We acknowledge support by the Hungarian Scientific Research Fund No. K72613, No. K73361, No. K101244, and No. CNK80991, by the New Széchenyi Plan No. TÁMOP-4.2.1/B-09/1/KMR-2010-0002, by the European Research Council Grant No. ERC-259374-Sylo, and by the Bolyai program of the Hungarian Academy of Sciences. J. C. acknowledges support from EU/FP7 under contract TEMSSOC and from ANR through Project No. 2010-BLANC-041902 (ISOTOP).

*dora@kapica.phy.bme.hu

[1] M. Z. Hasan and C. L. Kane, Rev. Mod. Phys. **82**, 3045 (2010).
[2] X.-L. Qi and S.-C. Zhang, Rev. Mod. Phys. **83**, 1057 (2011).
[3] C. L. Kane and E. J. Mele, Phys. Rev. Lett. **95**, 226801 (2005).
[4] B. A. Bernevig, T. L. Hughes, and S.-C. Zhang, Science **314**, 1757 (2006).
[5] C. Liu, T. Hughes, X.-L. Qi, K. Wang, and S.-C. Zhang, Phys. Rev. Lett. **100**, 236601 (2008).
[6] C. Weeks and M. Franz, Phys. Rev. B **82**, 085310 (2010).
[7] H.-M. Guo and M. Franz, Phys. Rev. B **80**, 113102 (2009).
[8] K. Sun, H. Yao, E. Fradkin, and S. A. Kivelson, Phys. Rev. Lett. **103**, 046811 (2009).
[9] L. Jiang, T. Kitagawa, J. Alicea, A. R. Akhmerov, D. Pekker, G. Refael, J. I. Cirac, E. Demler, M. D. Lukin, and P. Zoller, Phys. Rev. Lett. **106**, 220402 (2011).
[10] T. D. Stanescu, V. Galitski, J. Y. Vaishnav, C. W. Clark, and S. Das Sarma, Phys. Rev. A **79**, 053639 (2009).
[11] N. Goldman, I. Satija, P. Nikolic, A. Bermudez, M. A. Martin-Delgado, M. Lewenstein, and I. B. Spielman, Phys. Rev. Lett. **105**, 255302 (2010).
[12] M. König, S. Wiedmann, C. Brune, A. Roth, H. Buhmann, L. W. Molenkamp, X.-L. Qi, and S.-C. Zhang, Science **318**, 766 (2007).

[13] A. Roth, C. Bruene, H. Buhmann, L. Molenkamp, J. Maciejko, X.-L. Qi, and S.-C. Zhang, Science **325**, 294 (2009).
[14] I. Knez, R.-R. Du, and G. Sullivan, Phys. Rev. Lett. **107**, 136603 (2011).
[15] T. Kitagawa, E. Berg, M. Rudner, and E. Demler, Phys. Rev. B **82**, 235114 (2010).
[16] A. P. Schnyder, S. Ryu, A. Furusaki, and A. W. W. Ludwig, Phys. Rev. B **78**, 195125 (2008).
[17] X.-L. Qi, T. L. Hughes, and S.-C. Zhang, Phys. Rev. B **78**, 195424 (2008).
[18] A. Kitaev, AIP Conf. Proc. **1134**, 22 (2009).
[19] N. H. Lindner, G. Refael, and V. Galitski, Nature Phys. **7**, 490 (2011).
[20] J. Karch *et al.*, Phys. Rev. Lett. **105**, 227402 (2010).
[21] B. Wittmann *et al.*, Semicond. Sci. Technol. **25**, 095005 (2010).
[22] X.-L. Qi, T. L. Hughes, and S.-C. Zhang, Nature Phys. **4**, 273 (2008).
[23] See Supplemental Material at http://link.aps.org/supplemental/10.1103/PhysRevLett.108.056602 for further details.
[24] T. Oka and H. Aoki, Phys. Rev. B **79**, 081406 (2009).
[25] D. S. L. Abergel and T. Chakraborty, Nanotechnology **22**, 015203 (2011).
[26] J.-i. Inoue and A. Tanaka, Phys. Rev. Lett. **105**, 017401 (2010).
[27] Y. Zhou and M. W. Wu, Phys. Rev. B **83**, 245436 (2011).
[28] P. Hosur, Phys. Rev. B **83**, 035309 (2011).
[29] M. J. Schmidt, E. G. Novik, M. Kindermann, and B. Trauzettel, Phys. Rev. B **79**, 241306 (2009).
[30] H. Calvo, H. Pastawski, S. Roche, and L. Torres, Appl. Phys. Lett. **98**, 232103 (2011).
[31] T. Kitagawa, T. Oka, A. Brataas, L. Fu, and E. Demler, Phys. Rev. B **84**, 235108 (2011).
[32] H. Sambe, Phys. Rev. A **7**, 2203 (1973).
[33] *Quantum Transport and Dissipation*, edited by T. Dittrich, P. Hanggi, G.-L. Ingold, B. Kramer, G. Schon, and W. Zwerger (Wiley-WCH, Weinheim, 1998).
[34] A. M. J. Schakel and G. W. Semenoff, Phys. Rev. Lett. **66**, 2653 (1991).
[35] D. J. Thouless, Phys. Rev. B **27**, 6083 (1983).
[36] J. Cserti and Gy. Dávid, Phys. Rev. B **74**, 172305 (2006).